

Effects of different atomistic water models on the velocity profile and density number of Poiseuille flow in a nano-channel: Molecular Dynamic Simulation

H. Nowruzi¹, H. Ghassemi^{1,*}

¹Department of Maritime Engineering, Amirkabir University of Technology (Tehran Polytechnic), Hafez Ave, No 424, P.O. Box 15875-4413, Tehran, I. R. Iran

Received 17 December 2015;

revised 10 November 2016;

accepted 15 November 2016;

available online 24 December 2016

ABSTRACT: In the current study, five different atomistic water models (AWMs) are implemented, In order to investigate the impact of AWMs treatment on the water velocity profile and density number. For this purpose, Molecular dynamics simulation (MDS) of Poiseuille flow in a nano-channel is conducted. Considered AWMs are SPC/E, TIP3P, TIP4P, TIP4PFQ and TIP5P. To assessment of the ability of each model in prediction of velocity profile, it is compared with analytic velocity profile. Furthermore, MDS results of density number are evaluated by real non-dimensional value for density number of water (ρ^*). Based on computational results, predicted velocity profile from MDS is in appropriate accordance to analytic solution based on the Navier–Stokes equations. In addition, SPC/E and TIP4P models prepare the best prediction of the velocity profile, and are recommended where the averaged magnitude of velocity across the nano-channel is essential. Furthermore, a jump in velocity of TIP5P and TIP4P models is revealed in the vicinity of the nano-channel walls. However, approximately similar quantity is detected in the flow velocity of all different AWMs near the nano-channel walls. Finally, numerical results related to density number show, the TIP5P water model has higher compliance with the intended ρ^* , and thus this model is suggested, where density number plays an important role in our MDS.

KEYWORDS: Molecular dynamics simulation; Atomistic water models; Analytic solution; Velocity profile; Density number; Lennard-Jones;

Introduction

Water is known as the most popular liquid in the universe. Due to importance of water in nature, its properties are one of the most interested areas for scholar. However, In spite of more than a century study in the field of water; many unresolved questions remain beyond of this matter. Therefore, to comprehensive study on physicochemical characteristics and flow behavior of water, different AWMs are presented. Each model has specific features in parameter values and number of charge sites, which cause a various success in anticipating the accurate quantity and physical trend of a specific physical parameter.

On the other hand, among the water flow properties, its velocity profile and density number play an important role in many practical applications such as filtration by carbon-nanotubes (CNTs) [1-2], micro chemical reactors [3] and micro-nano electromechanical systems (MEMS/NEMS) [4]. So, it is important to select an appropriate atomistic water model in computer simulation such as molecular dynamics (MD) approach, which correctly predicts the real nature of the water. There are several studies related to the impressions of different AWMs on the fluid flow behavior, as discussed next. More research is done on the effects of water models on fluid flow viscosity [5-7].

For example, Markesteijn et al. [8] used MDS to show the effects of different atomistic water models on the viscosity-temperature relation. SPC/E, TIP4P, TIP4P/Ew, and TIP4P/2005 AWMs were employed in their study by considering Poiseuille flow inside a nano-channel. The error value they found for TIP4P/2005 as a best AWM for viscosity is lower than 8% against the experimental data. Guevara-Carrion et al. [9] carried out the numerical study on the impression of different AWMs to predict of several transport properties of pure liquid water and its mixtures with methanol and ethanol. By using SPC, SPC/E, TIP4P, and TIP4P/2005 model, they found that the TIP4P/2005 model performed better than the other models for all properties.

On the other hand, Lin et al. [10] examined numerically the Lennard-Jones and TIP4P models for flow characteristics of a plane Poiseuille flow in a nano-channel. They observed larger fluctuation in the velocity profile that induced by the TIP4P potential as compared to that induced by the LJ potential.

More recently, Plankova' et al. [11] investigated the effect of TIP4P/2005 model on density profile and surface tension of water vapor–liquid phase interfaces.

They used MDS and showed a proper accordance of this water model with real nature of the water. Also, Barbosa and Barbosa [12] by using MDS studied the density of the

*Corresponding Author Email: gaseemi@aut.ac.ir

Tel.: +982164543112; Note. This manuscript was submitted on December 17, 2015; approved on November 10, 2016; published online December 24, 2016.

Nomenclature			
AWMs	magnetic field strength (T)	l	Bond length [A^0]
SPC/E	specific heat at constant pressure	r_i	Position vector of point charge i
TIP3P	Similarity variable(= $Re_x^{1/2}(r^2 - r_o^2)/2r_o x$)	$q_{i\alpha}$	Charge of the α -th atom in the molecule i[e]
TIP4P	inertia coefficient of the porous medium (m^{-1})	$q_{j\beta}$	Charge of the β -th atom in the molecule j[e]
TIP4PFQ	Forchheimer parameter (= Fr_o)	r_{ij}^*	Dimensionless intermolecular distance Parameter
TIP5P	acceleration due to gravity ($m s^{-2}$)	r_c^*	Dimensionless cut-off radius
a_i	Grashofnumber (= $g\beta_f \Delta T l^3 / \nu_f^2$)	Greek Symbols	
F	thermal conductivity [$Wm^{-1}K^{-1}$]	σ	Atoms' diameter (characteristics length scale)
F_{ext}	Magnetic parameter(= $\sigma B_o^2 r_o / \rho_f u_{\infty}$)	ε	Characteristic potential energy
m	Conjugate heat transfer parameter (= $k_f / k_c \ln(r_o / r_i) Re^{1/2}$)	τ	Time unit
D	Prandtl number(= ν_f / α_f)	θ^0	HOH angle in TIP4P water model
p	inner and outer radii of the hollow cylinder (m)	φ^0	Oxygen- in TIP4P water angle
H	Reynolds number(= $u_{\infty} l / \nu_f$)	ε_0	Vacuum permittivity
N	Richardson number(= Gr / Re^2)	Δt	Time step
Y^*	temperature of the nanofluid (K)	μ_{dip}	Dipole moment
U^*	wall temperature (K)	μ	Shear viscosity
Rho^*	velocities in x and r directions, respectively ($m s^{-1}$)	ξ	Bulk viscosity
v^*	coordinates in axial and radial directions, respectively (m)	Subscripts	
T^*	Dimensionless temperature	ij	Considered parameter between two interacting molecules i and j
t^*	Dimensionless time unit	W	Water
K_B	Boltzmann constant	Pl	Platinum
F^*	Dimensionless force	1	Considered parameter between oxygen and q_1
		2	Considered parameter between oxygen and q_2

water molecules in the presence of hydrophobic and hydrophilic amino acids. For this purpose, they implemented SPC/E and TIP4P-2005 water models at $T=250K$ and $T=280K$. They showed an approximately similar behavior of these two models in prediction of density maximum.

Based on above cited works, it is detectable that several hypothetical atomistic water models have been presented on the water structure and its fluid flow behavior. However, there isn't any efficient numerical or experimental works on velocity profile and density number for different AWMs, which make it difficult to select an appropriate water model in MDS. Consequently, novelty of current study is related to report of impacts of different AWMs on the velocity profile and density number of flow in a nano-channel under a Poiseuille flow condition.

To this accomplishment, five different of water models such as SPC/E, TIP3P, TIP4P, TIP4PFQ and TIP5P are considered. On the other hand, Computational fluid dynamic (CFD) is regarded as an interested method to fluid flow study. Nevertheless, CFD is not proper and efficient for study of fluid flow under nano-scale. Because of lose out of continuum approximation and normally assumed linear constitutive relationships for fluid mechanic in CFD [13]. As a result, strong statistical mechanics method of DMS has suggested for study of nano-fluidic systems [14].

The following sections are organized as follows. AWMs are described in Section 2. Governing equations, methods and simulation details are explained in Section 3. Section 4 is given results and discussion and Section 6 is given for the conclusions.

Atomistic water models

Water molecule is composed of two hydrogen atoms connected to one oxygen atom. A schematic of water molecule configuration and some quantities to characterize its specific features is pictured in Figure 1.

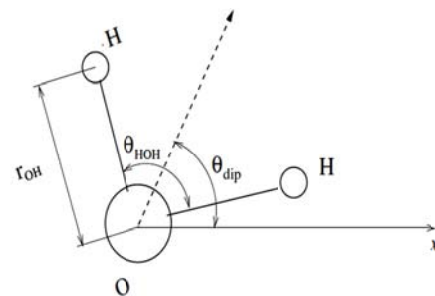


Fig. 1. Schematic of water molecule configuration

Based on Figure 1, in liquid state of water, bond length (r_{OH}) and bond angle (θ_{HOH}) are changed and modified by water-water interactions. On the other hand, due to higher

electro-negativity of oxygen atoms compared to hydrogen one, the negatively and positively charged sites will appear respectively for oxygen and hydrogen. Therefore, this charge difference cause to an electric dipole in the water molecule. Due to symmetric structure of water, dipole could present with a line started from oxygen and bisects of H-O-H angle [15-16]. In atomistic model of water with various point charge, dipole moment given by

$$\mu_{dip} = \sum_{i=1}^N q_i r_i \quad (1)$$

Where, N is the point charges number, q_i and r_i are charge and position vector of point charge i . Moreover, magnitude of μ_{dip} is related to length of the dipole vector. So, respect to the considered reference direction (x in Figure 1), the orientation of water is characterized by dipole angle θ_{dip} . As mentioned before, there are many atomistic water models (AWMs). However, in the current paper, the most commonly used and interested AWMs are considered and described briefly as following. Generally, planar and tetrahedral physical structure is detectable for different AWMs.

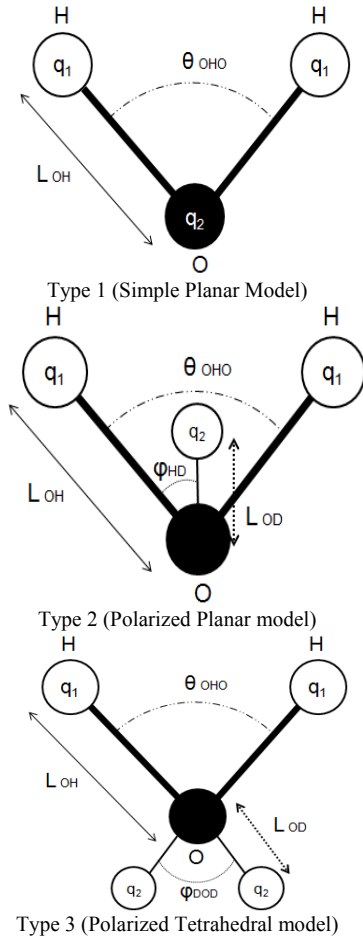


Fig. 2. Schematic illustration of parameter used for different atomistic water models (AWMs).

The schematic of these different structures are illustrated in Figure 2. As indicated by Figure 2, type 1 and 2 are planar and type 3 has a tetrahedral structure. Moreover, it is notable that, type 1 is the simplest water model and types 2 and 3 are polarized one. The reason of utilizing a polarizable water models is related to this fact that, water molecules in liquid state are all non-equivalent. In other words, due to their hydrogen bonding status, that affected by the arrangement of the neighbor water molecules, they are differing in their molecular orbital. Consequently, polarizable models (types 2 and 3 in Figure 2) are offered for better response to this phenomenon. However, in a simpler model (type 1 in Figure 2), formation of an 'average' structure is expected. Finally, all different AWMs are classified in these three physical structures. Common and interested of the AWMs are SPC/E, TIP3P, TIP4P, TIP4PFQ and TIP5P. SPC/E [17] is an extended simple point charge model that characterized by three point masses. In addition, TIP3P [18], TIP4P [19], TIP5P [20] are respectively, transferable intermolecular potential with 3, 4 and 5 points. TIP4PFQ [21] is a transferable intermolecular potential with 4 points and fluctuating charge model. TIP5P has the negatively charged interaction sites are located symmetrically along the lone-pair directions. As shown in Figure 2, the SPC/E and TIP3P models are type 1. In addition, TIP4P and TIP4PFQ are type 2 and TIP5P is classified in type 3. Main physical characteristics (based on specified parameters in Figure 2) and Lennard-Jones parameters of considered AWMs are tabulated in Table.1.

Table 1

Main physical characteristics (based on specified parameters in Figure 2) and Lennard-Jones parameters of AWMs [15-21].

Physical Characteristic	SPC/E	TIP3P	TIP4P	TIP5P	IP4PFQ
Type of AWM	1	1	2	3	2
σ [Å]	3.166	3.15061	3.15365	3.12000	3.15365
ϵ [kJ mol ⁻¹]	0.650	0.6364	0.6480	0.6694	0.6480
L_{OH} [Å]	1.0000	0.9572	0.9572	0.9572	0.9572
L_{OD} [Å]	---	---	0.15	0.70	0.15
θ_{OHO} [deg]	109.47	104.52	104.52	104.52	104.52
ϕ_{HD} [deg]	---	---	52.26	---	52.26
ϕ_{DOD} [deg]	---	---	---	109.47	---
q_1 [e]	+0.4238	+0.4170	+0.5200	+0.2410	+0.63 (Ave)
q_2 [e]	-0.8476	-0.8340	-1.0400	-0.2410	1.26 (Ave)
τ [Ps]	1.66674	1.67627	1.66280	1.61855	1.66280
Velocity unit (σ/τ) [Å/Ps]	1.899	1.879	1.896	1.927	1.896
Temperature unit (ϵ/k_B) [k]	78.844	77.194	78.601	81.197	78.601

In Table 1, σ , ϵ , τ are respectively, atoms diameter (characteristics length scale), parameter that governs on the strength of interactions (characteristic potential energy) and time unit, which we use them in Lennard-Jones potential in the next section.

Methods and Simulation Details

Governing Equation

As previously mentioned, MDS is performed for current study. The nature of this method is a Lagrangian based that locations of molecules is measurable in consecutively by using Newtonian's equations of motion. For this purpose, at first the applied forces on each molecule are calculated.

Second, their new location and velocities in a next time step will be obtained by combining with a current location and velocity of each molecule. This procedure will be repeated in each step.

In deterministic scheme of MDS, molecule interacted together with intermolecular potential of U . We know the equation of motion for a molecule i without any moment of inertia and rotationally symmetrical is

$$m_i a_i = F_i \quad (2)$$

where, F_i shows an overall force acts on the molecules by using

$$F_i = \sum_{j_w \neq i, j=1}^N F_{ij} + \sum_{j_w \neq i, j=1}^{N_w} F_{ijw} + F_{ext} \vec{i} \quad (3)$$

Here, \vec{i} shows a unit vector in flow direction. The first term in hand side of equation 3 represents an intermolecular force based on potentials between molecule i and other fluid molecules in the computational domain. Also, second and third terms of equation 3 shows force between molecule i with all wall particles j and external force, respectively.

A single molecule will be affected by intermolecular potential energy functions of every molecule in the system including bonded and non-bonded neighbors. Hence, the affecting intermolecular potential on each water molecule is including bonded and non-bonded potentials. In the present study, non-bonded potential is considered [16].

Each non-bonded potential are formed from two potential parts: Van-der-waals and electrostatic. In the current paper, Lennard-Jones (LJ) 6-12 potential (as short-range repulsive/long-range attractive potential [14,22]) is implemented as the Van-der-waals potential. This potential is used for fluid-fluid and fluid-solid wall atoms (in fixed/frozen sate [23]) interactions. Moreover, to realistic modeling of water molecules, we employ electrostatic force, based on Coulomb's law. Impression of the partial charges on the interaction sites respond to the electrostatic

field of the molecules is the reason of adding electrostatic to our intermolecular potential.

Simulation details

For MDS of different AWMs in nano-channel, non-equilibrium and paralleled MD solver of *mdFoam* in Open source software of OpenFOAM is modified and performed. Based on other study in field of MDS [24-27], this solver has an appropriate capability in MDS. Also, to decrease of computational cost and better inference of readers from the computational results, as usual for MDS, reduced units are implemented. The defined quantities in reduced unite system is presented in Table 2.

Table 2

Defined quantities for MDS in reduced unit.

Quantity	Reduced Unit
Diameter (Υ^*)	Y/σ
Energy (J^*)	E/ϵ
Density (Rho^*)	$\rho\sigma^3$
Velocity (v^*)	$v/(\sigma/\tau)$
Temperature (T^*)	$T/(\epsilon/k_B)$
Time (t^*)	$t/(m^{0.5}\sigma/\epsilon^{0.5})$
Force (F^*)	$F/(\epsilon/\sigma^2)$

According to reduced unit, the general form of dimensionless potential is

$$U^*(r_{ij}^*) = 4 \left[\left(\frac{1}{r_{ij}^*} \right)^{12} - \left(\frac{1}{r_{ij}^*} \right)^6 \right] + \sum_{\alpha=1}^3 \sum_{\beta=1}^3 \frac{q_{i\alpha} q_{j\beta}}{4\pi\sigma_{O\alpha O\beta} \epsilon_{O\alpha O\beta} \epsilon_0 r_{i\alpha, j\beta}^*} r_{ij}^* \leq r_c^* \quad (4)$$

Parameters in the equation 4 are described at Nomenclature. The first term of equation 4 is a force field that related to Lennard-Jones (LJ) 6-12 for non-bonded oxygen-oxygen potential. Second term is also associated with the electrostatic force based on Coulomb's Law. Also, we set the value of 2.5 for dimensionless cutoff radius (r_c^*) [22]. On the other hand, the platinum metal is used as a solid wall of a nano-channel. Lennard-Jones potential parameters for this metal are $\sigma_{Pl} = 2.95[\text{\AA}]$ and $\epsilon_{Pl} = 2.128 [\text{kJ mol}^{-1}]$ [28].

It must be mentioned that, Face-Centered-Cubic (FCC) mesh structure is performed for all molecules' arrangement in this paper. The reason of this selection is related to the real physical structure of liquid and solids in nature [29].

Based on statistical thermodynamics, for initial velocity distribution in the equilibrium isolated system with fix temperature, Maxwell-Boltzmann is considered as

$$p(v_{iz}) = \left(\frac{m_i}{2\pi k_B T} \right)^{0.5} \exp \left[-\frac{1}{2} \frac{m_i v_{iz}^2}{k_B T} \right] \quad (5)$$

Prediction of possibility of velocity of v_{iz} for a molecule i with mass of (m_i) at temperature of T is the interpretation of equation 5. The initial velocities set to such that the momentum of whole system is zero.

Schematic of computational domain is illustrated in Figure 3.

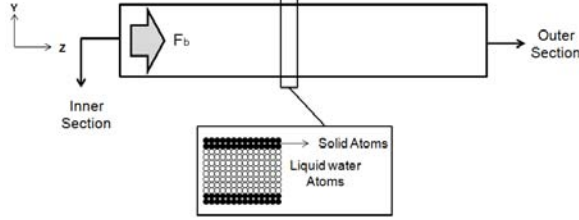


Fig. 3. Schematic of the computational domain in MDS. In total 4817 water molecules are placed between two solid atomistic walls each consisting of 878 platinum molecules in two layers. Poiseuille flow is generated by a body force F_b in the Z-direction

As observed in Figure 3, physical domain is extending $32\sigma_{SPC/E}$ in length (Z-direction). Also, height of nano-channel in Y-direction is $H=9.5\sigma_{SPC/E}$.

Additionally, as can be seen in Figure 3, to construct of nano-channel walls, double layers of platinum molecules are implemented.

Also, to omission of unwanted wrap-around in computational domain, periodic boundary condition is used. This boundary condition (BC) with feature of infinite number of copies of system around of itself is a confirmed BC in MD modeling [30]. Consequently, we applied this BC in the direction of fluid flow (Z-Direction).

In order to apply the Poiseuille flow to our computational domain, water flow is driven by a constant external body force of $F_{ext}=F_b=2.27 e^{-9} \epsilon/\sigma^2$ on the all molecules along the Z-direction at $P=1\text{atm}$.

For sampling procedure, twenty independent equal segments (bins) are placed across the Y-direction. Then, stochastic averaging is applied on molecular dynamic data in each bin to extract of macroscopic properties of velocity profile and number density of water flow. Due to use of Berendsen thermostat, all simulations are done in the intended fixed temperature of $T^*=3.73$. Moreover, the density number of simulations are considered as $\text{Rho}^*=\rho\sigma^3=0.998$.

Paralleled code on a core I Eight CPUs with RAM of 6GB is performed in this work. Also, Molecular dynamic equations are solved by time step of $\Delta t=6 \times 10^{-4} \tau$. This time interval (Δt), due to real-time of 6.4fs and 3.1fs for H-O-H bend and O-H stretch, is small enough to make sure numerical stability [10].

Real run time for each case is about $5 \times 10^3 \tau$ to simulate of 1ns of the problem until stability achievement including equilibrium process by NVT ensemble and Poiseuille flow simulation.

Continued, the results of velocity profile and density number for different AWMs are presented.

Results and Discussion

Five different AWMs are employed for this simulation, for which the parameters can be found in Table 1. During the simulation, the velocity profile and density number values are collected throughout the bins. At the beginning of this section, computed velocity profiles of different AWMs under Poiseuille flow from MDS are compared with analytical solution. Then the density number is analyzed for various AWMs.

Velocity profile of different AWMs vs. analytical solution

Lack of experimental study related to our work was observable from literature review. As a result, similar to other study [31-32], we use analytical solution for velocity profile of Poiseuille flow in nano-channel to compare it by different intended AWMs simulations. Therefore, following derivation is performed for extract of analytical velocity profile.

As indicated by Figure 3, consider a water fluid confined between two parallel plate at rest that located at $y=\pm H/2$ in orthogonal manner to Y-direction (Poiseuille flow [33]), where in addition of external force of $F=F_{ext} \hat{z}$, a pressure gradient $\partial p/\partial z$ exist in Z-direction, then balance equation for momentum is

$$\frac{\partial \mathbf{u}}{\partial t} + \frac{1}{\rho} \nabla \cdot \mathbf{P} + \mathbf{u} \cdot \nabla \mathbf{u} - \mathbf{F} = 0, \quad (6)$$

Here, \mathbf{u} is flow velocity, ρ as density and \mathbf{p} is a tensor of pressure. In this case, Navier-Stokes equation can be obtained as

$$\mathbf{P}_{ij} = p\delta_{ij} - \mu \left(\frac{\partial u_i}{\partial z} + \frac{\partial u_j}{\partial z} - \frac{2}{3} \delta_{ij} \nabla \cdot \mathbf{u} \right) \quad (7)$$

$$-\xi \delta_{ij} \nabla \cdot \mathbf{u},$$

Here, μ and ξ are shear viscosity and bulk viscosity, respectively.

Due to this fact that, in Poiseuille flow, $\partial u/\partial t = 0$ and $\mathbf{u}(\mathbf{r})=\mathbf{u}(y) \hat{z}$, as a result, new form of Navier-Stokes equation for Poiseuille flow is

$$\frac{\partial p}{\partial y} = 0, \quad \frac{\partial^2 \mathbf{u}}{\partial y^2} = \frac{1}{\mu} \left(\frac{\partial p}{\partial z} - \rho F_{ext} \right). \quad (8)$$

Solution of above equation for no-slip boundary condition (zero velocity near the walls) now becomes

$$u(y) = -\frac{1}{2\mu} \left(\rho F_{ext} - \frac{\partial p}{\partial z} \right) \left(y^2 - \frac{H^2}{4} \right). \quad (9)$$

Equation 9 is representative of Poiseuille flow. However, it is noticeable that, $\partial p/\partial z = 0$ in the current study. Indeed, this body force is not based on the pressure gradient because the system is able to remain longitudinally

homogeneous. In addition, as mention before, water flow is driven by a constant external body force equal to $F_{ext}=F_b=2.27e^{-9}\epsilon/\sigma^2$ on the all molecules along the Z-direction at P=1atm.

Figure 4 shows the velocity profile across the channel for different AWMs compare to Analytical U^* .

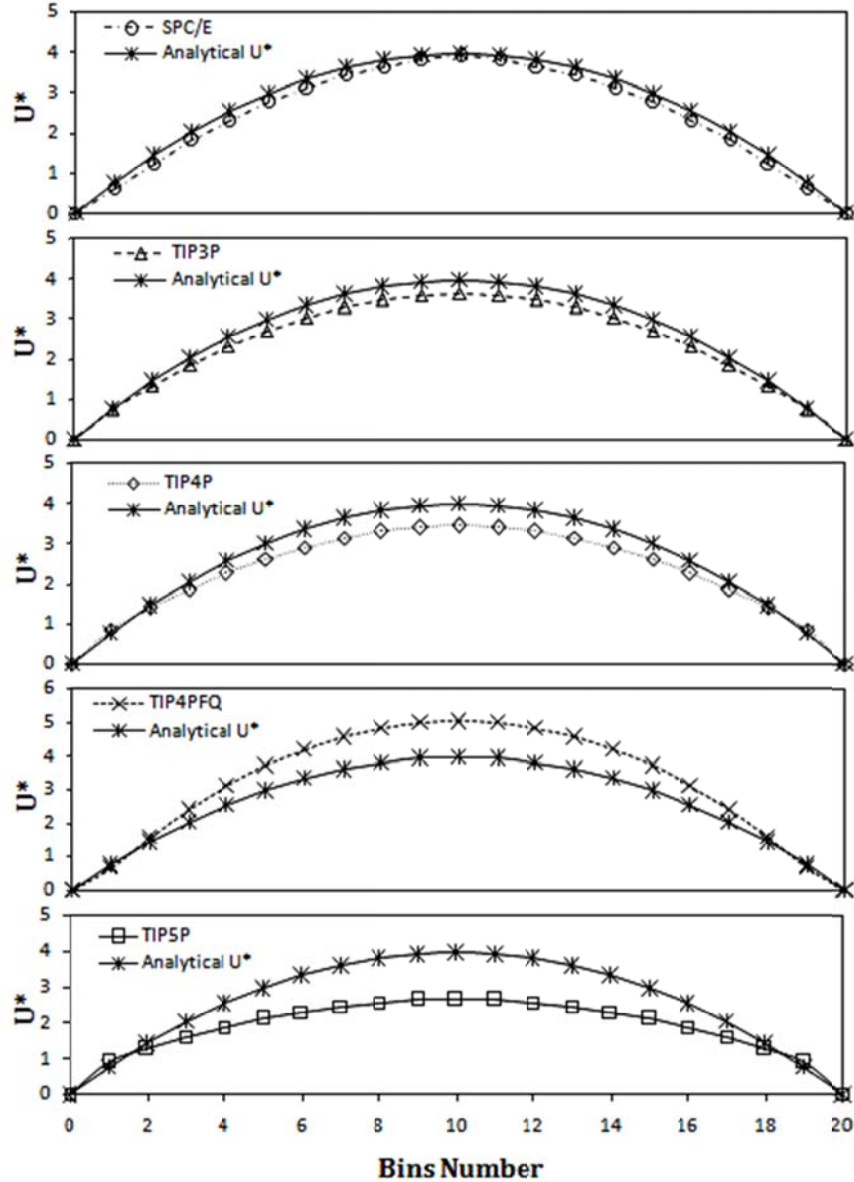


Fig. 4. Velocity Profile of different AWMs vs. analytical velocity profile in a nano-channel under Poiseuille flow

Based on Figure 4, as expected, the computed velocity profiles from MD have similar trend (second-order polynomial) to the analytical solution based on the Navier–Stokes equations, for all cases. However, for all AWMs, a

minor difference in convexity radius of parabolic trend of velocity profile compared to analytical solution is observable. Also, maximum error of velocity profile can be seen at the peak of the velocity profile in centerline of the

nano-channel. In addition, velocity profile of SPC/E, TIP3P, TIP4P and TIP5P water models have lower value compared to analytical solution, especially for TIP5P, Whereas, TIP4PFQ water model show significant higher value rather than the analytic. In addition, best fitting to analytical data of velocity profile is detectable for SPC/E water model. Moreover, TIP5P water model has the most value in velocity profile gradient. Consequently, it is deduced that, there is not a constant shear stress along the nano-channel for this model.

Detailed difference between overall averaged of the velocity across the bins for difference AWMs compared to analytical solution is summarized in Table 3.

Table 3

Detailed difference between velocity averages of different AWMs compared to analytical solution.

Atomistic water models	$U_{AWMs}^* - U_{Analytical}^*$
SPC/E	-6.49%
TIP3P	-8.54%
TIP4P	-11.66%
TIP4PFQ	+23.43%
TIP5P	-27.71%

(-) lower value compared to Analytical Velocity profile

(+) Higher value compared to Analytical Velocity profile

Obtained differences in Table 3 confirm this conclusion; the TIP5P and TIP4PFQ under-predict the velocity profile by as much as -27.71% and +23.43 %, respectively. As a result, this two water models are unacceptable AWMs rather than analytic. Also, TIP4P and TIP3P under-predict the velocity profile by -11.66% and -8.54%, respectively. Finally, SPC/E water model under-predicts the velocity profile only with -6.49%. Consequently, SPC/E water model is recommended for velocity profile prediction under Poiseuille flow in nano-channel.

Figure 5 is presented for better comparison between different AWMs velocity profile. As can be seen in Figure 5, for Bins Number in interval of [2-18], as discussed formerly, TIP5P, TIP4P, TIP3P, SPC/E and TIP4PFQ, respectively have lower to higher value of U^* . However, at intervals of Bins Number = [0-2 & 18-20], which are representative of regions close to the nano-channel walls; behavior of velocity profile of AWMs has been changed. Indeed, a jumping variation to higher value is observable for TIP5P and TIP4P. The reason of this variation can be found in the interaction between water molecules with the nano-channel wall atoms. Finally, approximately similar value of U^* is recognizable for SPC/E, TIP3P and TIP4P in intervals of Bins Number = [0-4 & 16-20].

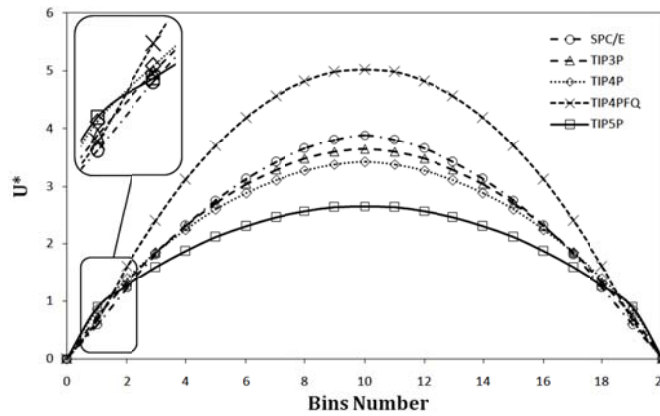


Fig. 5. Velocity profile for different AWMs

Density number of different atomistic water model

Figure 6 shows density number across a nano-channel obtained from different AWMs simulations under Poiseuille flow.

As it is shown in Figure 6, density number profile has remarkable fluctuations near the nano-channel wall for all different AWMs. These fluctuations are oscillated around a higher or lower constant value in the center of the nano-channel. These fluctuations are the result of molecular interaction between solid walls atoms and water flow molecules. This physical phenomenon is also observed in experiment [34].

On the other words, Based on Figure 6, three significant variations in behavior of the density number is observable.

Peaks, troughs and oscillation around constant density number are these three notable phenomena. Peaks and troughs in density number are due to layering procedure.

Due to greater equilibrium between nano-channel wall and neighboring water molecules compared to elsewhere, water molecules will be placed in dense layers parallel to nano-channel walls. The peaks of density number are revealed the situation of these layers, because powerful repulsion in Lennar-Jones potential leads to minimal distance in Y-direction for Oxygen atoms.

In addition, troughs in the density number profile, is due to smaller number of molecules. Reduction of water molecules surrounding the dense layer is related to avoiding

of water molecules in approaching to dense layer with strong repulsion.,

Oscillation around constant density number is another phenomenon in density number of water flow in a middle

of nano-channel. The reason of this fact is due to increase of disorder in water molecules, so an isotropic treatment with higher or lower oscillation around constant density number is occurred.

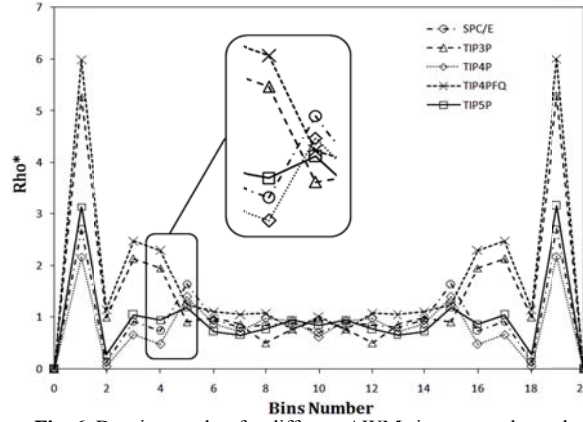


Fig. 6. Density number for different AWMs in a nano-channel

On the other hand, larger peak in density number value is evident for TIP4PFQ, TIP3P, TIP5P, SPC/E and TIP4P, respectively. Also, it is noticeable that, larger peak leads to momentum increment and as a result, wall resistance will be decreased. Also, based on enlarge zone of Figure 6, it is visible that, oscillation to higher value in Rho^* for TIP4PFQ and TIP3P and to lower value for SPC/E, TIP4P and TIP5P is observable in Bins Number= [5-4 & 15-20]. Therefore, it can be concluded that, density number in approximately 50% of cross-section of nano-channel is strongly affected by wall atoms. Finally, with comparison of average density number for different AWMs compared to real density of water at $T^*=3.73$ that is $Rho^* = \rho\sigma^3 = 0.998$, TIP5P, SPC/E water model have the best fitting to this value, respectively. Also, due to lack of appropriate prediction (high fluctuation) of density number for TIP4PFQ, this water model isn't recommended for MDS that density number play an important role.

Conclusion

In study of water flow behavior in nano-channels, velocity profile and density number play an important role. Also, in MDS of water flow in nano-scale, different AWMs are presented by scholars. However, structural difference among AWMs is impressive on the accuracy of velocity profile and density number.

Consequently, in the current study, the effects of five different AWMs on the velocity profile and density number are investigated. This was accomplished by simulating Poiseuille flow in a MD nano-channel. In addition, SPC/E, TIP4P, TIP3P, TIP4PFQ and TIP5P are intended atomistic water models. To evaluate of the accuracy of velocity profile for each AWM, it is compared to analytical solution. Also, the density number for different AWMs is analyzed with its real non-dimensional density value at $T^*=3.73$.

Extracted results of velocity profile showed that, computed velocity profile by MDS is in good agreement with the analytical solution for all cases. However, the SPC/E water model gives the best anticipation of the velocity profile compared to analytical solution. Also, the TIP4P and TIP3P water models have nearly homologous prediction of velocity profile with moderate variations compared to analytic.

While the TIP5P and TIP4PFQ as an inappropriate AWMs, predict the velocity profile than the analytical solution by difference of -27.71% and +23.43 %, respectively. As a result, in MDS which velocity profile is a significant parameter, the SPC/E water model is suggested. It must be noted that, near the walls, all different AWMs have approximately similar value. Also, in the vicinity of the nano-channel wall, a jump in velocity of TIP5P and TIP4P is observed.

On the other hand, among the most important extracted findings related to density number, TIP4PFQ and TIP4P water model respectively have higher and lower peak in density number value. Moreover, density number in half of the nano-channel cross-section is strongly impressed by wall atoms, for all different AWMs. Finally, with comparison between real non-dimensional density ($Rho^* = \rho\sigma^3 = 0.998$) with averaged density number for different AWMs, one can be concluded that, TIP5P and SPC/E water models with better accordance to the intended Rho^* , are the preferred models.

At the end, it is noticeable that, detailed parameter including, properties of nano-channel wall, different temperature, or size of the system are impressive on the velocity profile and density number of different AWMs. Consequently, the effects of these parameters on the velocity profile and density number of different AWMs is exciting enough to conduct our future study.

References

- [1] B. Lee, Y. Baek, M. Lee, D. H. Jeong, H. H. Lee, J. Yoon, Y. H. Kim: A carbon nanotube wall membrane for water treatment, *Nature Communications* 6 (2015).
- [2] R. Das, M.d. E. Ali, S. B. A. Hamid, S. Ramakrishna, Z. Z. Chowdhury : Carbon nanotube membranes for water purification: A bright future in water desalination, *Desalination* 36 (2014) 97–109.
- [3] R. Saidur, K.Y. Leong, H.A. Mohammad : A review on applications and challenges of nanofluids, *Renewable and Sustainable Energy Reviews* 15 (2011) 1646–1668.
- [4] A. C. Fischer, F. Forsberg, M. Lapisa, S. J. Bleiker, G. S.N. Roxhed, F. Niklaus: Integrating MEMS and ICs, *Microsystems & Nanoengineering* (2015).
- [5] S. Yongli, S. Minhua, C. Weidong, M. Congxiao, L. Fang: The examination of water potentials by simulating viscosity, *Computational Materials Science* 38 (2007) 737–740.
- [6] Y. Song, L. Dai: The shear viscosities of common water models by non-equilibrium molecular dynamics simulations, *Molecular Simulation* 36 (2010) 560-567.
- [7] M. González, J. Abascal: The shear viscosity of rigid water models, *J. Chemical Physics* 132 (2010) 096101.
- [8] A. P. Markesteijn, R. Hartkamp, S. Luding, J. Westerweel : A comparison of the value of viscosity for several water models using Poiseuille flow in a nano-channel , *J. Chemical Physics* 136 (2012) 134104.
- [9] G. Guevara-Carrion, J. Vrabc, H. Hasse: Prediction of self-diffusion coefficient and shear viscosity of water and its binary mixtures with methanol and ethanol by molecular simulation, *J. Chemical Physics* 134 (2011) 074508.
- [10] D. T. W. Lin, C. K. Chen: A molecular dynamics simulation of TIP4P and Lennard-Jones water in nanochannel, *Acta Mechanica* 173 (2004) 181–194.
- [11] B. Plankova, V. Vins, J. Hruby, M. Duska, T. Neme, D. Celny: Molecular simulation of water vapor–liquid phase interfaces using TIP4P/2005 model, *EPJ Web of Conferences* 92 (2015).
- [12] R. d. C. Barbosa, M. C. Barbosa: Hydration shell of the TS-Kappa protein: higher density than bulk water, *Physica A: Statistical Mechanics and its Applications* 439 (2015) 48–58.
- [13] J.S. Hansen and J. T. Ottesen, Molecular dynamics simulations of oscillatory flows in microfluidic channels, *J. of Micro Fluidic and Nano Fluidic* 2 (2006) 301-307.
- [14] D. C. Rapaport: *The art of molecular dynamics simulation*, Cambridge, New York (2004).
- [15] G. Karniadakis, A. Beskok, Narayan Aluru: *Microflows and nanoflows fundamentals and simulation*, Springer, New York (2005).
- [16] http://www1.lsbu.ac.uk/water/water_models.html.
- [17] H. J. C. Berendsen, J. R. Grigera, T. P. Straatsma: The missing term in effective pair potentials, *J. Physical Chemistry* 91 (1987) 6269-6271.
- [18] W. L. Jorgensen, J. Chandrasekhar, J. D. Madura, R. W. Impey, M. L. Klein: Comparison of simple potential functions for simulating liquid water, *J. Chemical Physics* 79 (1983) 926-935.
- [19] W. L. Jorgensen, J. D. Madura: Temperature and size dependence for monte carlo simulations of TIP4P water, *Mol. Phys* 56 (1985) 1381-1392.
- [20] M. W. Mahoney, W. L. Jorgensen: A five-site model for liquid water and the reproduction of the density anomaly by rigid, nonpolarizable potential functions, *J. Chemical Physics* 112 (2000) 8910-8922.
- [21] S. W. Rick: Simulation of ice and liquid water over a range of temperatures using the fluctuating charge model, *J. Chemical Physics* 114 (2001) 2276-2283.
- [22] M. Allen, D. Tildesley: *Computer simulation of liquids*, Oxford University Press (1987).
- [23] P.A. Thompson, S.M. Troian: A general boundary condition for liquid flow at solid surfaces, *Nature* 389 (1997) 360–2.
- [24] G. B. Macpherson, M. K. Borg, J. M. Reese: Generation of initial molecular dynamics configurations in arbitrary geometries and in parallel, *Mol. Simul* 33 (2007) 1199–1212.
- [25] G.B. Macpherson, J. M. Reese: Molecular dynamics in arbitrary geometries: parallel evaluation of pair forces, *Mol Simul* 34 (2008) 97–115.
- [26] G. B. Macpherson, N. Nordin, H. G. Weller: Particle tracking in unstructured, arbitrary polyhedral meshes for use in CFD and molecular dynamics, *Commun. Numer. Methods Eng* 25 (2009) 263–273.
- [27] M.K. Borg, G.B. Macpherson, J.M. Reese: Controllers for imposing continuum-to molecular boundary conditions in arbitrary fluid flow geometries, *Mol Simul* 36 (2010) 745–57.
- [28] H. J. C. Berendsen, J. R. Grigera, T. P. Straatsma : The missing term in effective pair potentials, *J. Physical Chemistry* 91(1987) 6269-6271.
- [29] R. Kamali, P. Radmehr, A. Binesh: Molecular dynamics simulation of electro-osmotic flow in a nanonozzle, *Micro & Nano Letters* 7 (2012) 1049–1052.
- [30] J. P. Hansen, I. R. McDonald: *Theory of simple liquids*, Academic Press (2006).
- [31] W. A. Khan, M. M. Yovanovich: *Analytical Modeling of Fluid Flow And Heat Transfer In Micro/Nano-Channel Heat Sinks: Proceedings of IPACK2007, ASME Interpack '07, Vancouver, British Columbia, CANADA (2007).*

- [32] A. S. Ziarani, A. A. Mohamad: A molecular dynamics study of perturbed Poiseuille flow in a nanochannel, *Microfluid Nanofluid* 2 (2005) 12–20.
- [33] R. B. Bird, W. E. Stewart, E. W. Lightfoot: *Transport phenomena*, Wiley, New York (1960).
- [34] D.Y.C. Chan, R.G Horn: The drainage of thin liquid films between solid surfaces, *J. Chemical Physics* 83 (1985) 5311-5324.